Journal of Hazardous Materials 182 (2010) 191–196

Contents lists available at ScienceDirect

Journal of Hazardous Materials

journal homepage: www.elsevier.com/locate/jhazmat

Man-made vitreous fiber produced from incinerator ash using the thermal plasma technique and application as reinforcement in concrete

Sheng-Fu Yang*, To-Mai Wang, Wen-Cheng Lee, Kin-Seng Sun, Chin-Ching Tzeng

Atomic Energy Council, Institute of Nuclear Energy Research, Taoyuan, Taiwan, ROC

ARTICLE INFO

Article history:
Received 26 February 2010
Received in revised form 14 May 2010
Accepted 2 June 2010
Available online 9 June 2010

Keywords:
Thermal plasma technology
Incinerator ash
Man-made vitreous fiber
Fiber-reinforced concrete

ABSTRACT

This study proposes using thermal plasma technology to treat municipal solid waste incinerator ashes. A feasible fiberization method was developed and applied to produce man-made vitreous fiber (MMVF) from plasma vitrified slag. MMVF were obtained through directly blending the oxide melt stream with high velocity compressed air. The basic technological characteristics of MMVF, including morphology, diameter, shot content, length and chemical resistance, are described in this work. Laboratory experiments were conducted on the fiber-reinforced concrete. The effects of fibrous content on compressive strength and flexural strength are presented. The experimental results showed the proper additive of MMVF in concrete can enhance its mechanical properties. MMVF products produced from incinerator ashes treated with the thermal plasma technique have great potential for reinforcement in concrete.

1. Introduction

Vitrification to treat municipal solid waste incinerator (MSWI) ashes has attracted much attention [1–8], especially in countries with high population densities in metropolitan areas and very limited space available for waste disposal. Thermal plasma treatment is one of the best methods of vitrification. In thermal plasma vitrification, the heat generated by the plasma is adopted to treat MSWI ashes containing heavy metals, inorganic and/or organic substances to temperatures of 1400–1600 °C. During treatment, the organic contaminants are thermally destroyed and the inorganic substances are melted to generate vitrified slag through a water-quenched unit.

Recycling is an economical and environmentally friendly way to handle some types of hazardous wastes, reducing the amounts disposed in landfills. Generally, vitrified slag was applied to construction materials including roadbed aggregate, asphalt concrete, cement, permeable bricks and glass ceramics [8–11]. This study was conducted to find alternative applications for vitrified slag. One such possible application is to manufacture man-made vitreous fiber (MMVF) or man-made mineral fiber (MMMF) from them. The fiber blowing process was adopted to produce fibers when the melted mass was broken with high velocity compressed air. In this paper, the development of a manufacturing method was initiated for concrete-reinforcing MMVF. The basic technological characteristics of fiber, including morphology, diameter, shot content, length and alkaline resistance, are described in the following sections.

Fibers are used in concrete as reinforcement materials from an extensive array of materials, including steel, polyethylene terephthalate, nylon, polypropylene, glass and ceramic. Previous studies demonstrated they can improve the mechanical properties of concrete such as compressive strength, flexural strength, impact strength and toughness [12–15]. There are no related studies utilizing MMVF from MSWI ashes as the reinforcement in concrete until now. In this paper, the performance of MMVF-reinforced concrete in compressive strength and flexural strength were investigated and reported.

2. Materials and methods

2.1. Plasma vitrified slag

The 250 kg/h pilot-scale plasma (1.2 MW transferred plasma torch) melting system was constructed in the Institution of Nuclear Energy Research (INER) to treat fly ash and bottom ash from municipal solid waste incinerators. During the plasma vitrified process, the melted incinerator ashes (MSWI fly ash and bottom ash at a weight ratio of 1:1) were continuously discharged into the water-quenching unit to generate water-quenched plasma vitrified slag. The color of vitrified slag was deep black, with a particle size in the range of 0.4–18.0 mm and d_{50} was 3.0 mm. The average true density and hardness (Mohs) of water-quenched slag are 2.85 g/cm and 3–4, respectively.

* Corresponding author at: No. 1000, Wenhua Rd., Jiaan Village, Longtan Township, Taoyuan County 32546, Taiwan, ROC. Tel.: +886 3 4711400x3870; fax: +886 3 4115617.
E-mail addresses: sfyang@iner.gov.tw, d95541006@ntu.edu.tw (S.-F. Yang).

0304-3894/$ – see front matter © 2010 Elsevier B.V. All rights reserved.
doi:10.1016/j.jhazmat.2010.06.014

2.2. Characterization methods of the MSWI ashes and vitrified slag

The chemical compositions of MSWI fly ash, bottom ash and water-quenched vitrified slag were determined by inductively coupled plasma mass spectrometry (ICP-MS) (X Series II; Thermo, USA). Before the digestion of solid specimens, the bottom ash and vitrified slag were crushed, ball milled and passed through U.S.A. Standard Sieves (Nos. 100). The powdered fly ash, bottom ash and vitrified slag were digested with HF/HCl/HNO_3 acidic solution in the microwave digester. Afterward inorganic constituents following digestion in acidic digestion were confirmed by ICP-MS.

The chlorine values were determined by heating the MSWI fly ash, bottom ash and vitrified slag in a tube furnace with oxygen. A weighed sample (1.0 g) was burned in a tube furnace at an operating temperature of 850 °C in a stream of oxygen. During combustion, chlorine in the sample was released as Cl_2 and then was absorbed into a solution of 3% hydrogen peroxide (H_2O_2) where it dissolved forming dilute solution of hydrochloric (HCl) acid. The quantity of chlorine presented in absorption solution was analyzed by ion-exchange chromatography. Afterward the percentage of chlorine contained in the solid specimens can be calculated.

The vitrified slag was ball milled and passed a 75 μm (No. 200) sieve. The test specimen was shaped in a cone mold and subsequently placed it into the electric furnace to observe the deformation of cone at temperatures of 1100–1200 °C. The softening point of vitrified slag was defined as the temperature at which triangular pyramid fused down and the height was equal to the width at the base as showed by American society for testing material (ASTM) D1857-04 [16].

2.3. Producing mineral fiber

In this work, the laboratory scale device (3.5 kg per batch) was created to produce mineral fiber. Fig. 1 shows the design of a melting furnace. It mainly consists of dual batch feeding, an electrically heated furnace (heating element: molybdenum silicide, $MoSi_2$) and a fiber blowing unit. The furnace is lined with refractory materials and the melting temperature was controlled by a programmable logic controller (maximum temperature: 1600 °C). The fiber blowing unit is comprised of a compressed air system (air generator and tank) and blowing nozzle (Fig. 2). The diameter of the blowing

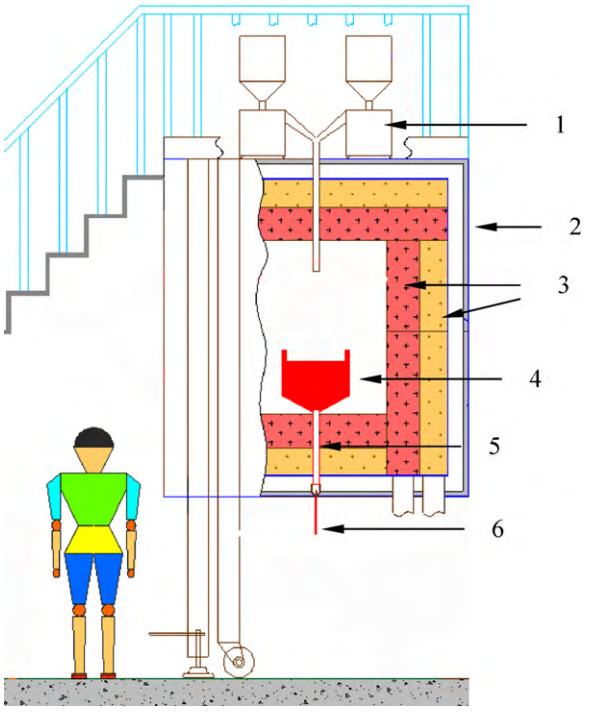

Fig. 1. Scheme of a melting furnace. (1) Batch feeding; (2) melting furnace; (3) insulating materials; (4) Al_2O_3 crucible; (5) throat; (6) oxide melt stream.

nozzle is 50 mm with seven interior openings. The central one has a diameter of 4 mm and the rest are 2.5 mm with a 20° angle. The purpose of designing this kind of blowing nozzle was to concentrate compressed air and achieve a high velocity to break the melting material into small particles, and then attenuate those particles into mineral fibers. Fig. 3 presents procedures for manufacturing mineral fiber. Plasma vitrified slag is put in feeding hoppers to be fed into the crucible by an automatic vibration mechanism or directly put in the crucible. The capacity of plasma vitrified slag for each batch was 3.5 kg. The starting material was processed with heat to obtain the melting material in a furnace at 1600 °C. Then, the temperature of the furnace is adjusted and fixed at a 1480 °C. The viscosity of the melting material in the crucible at this point is

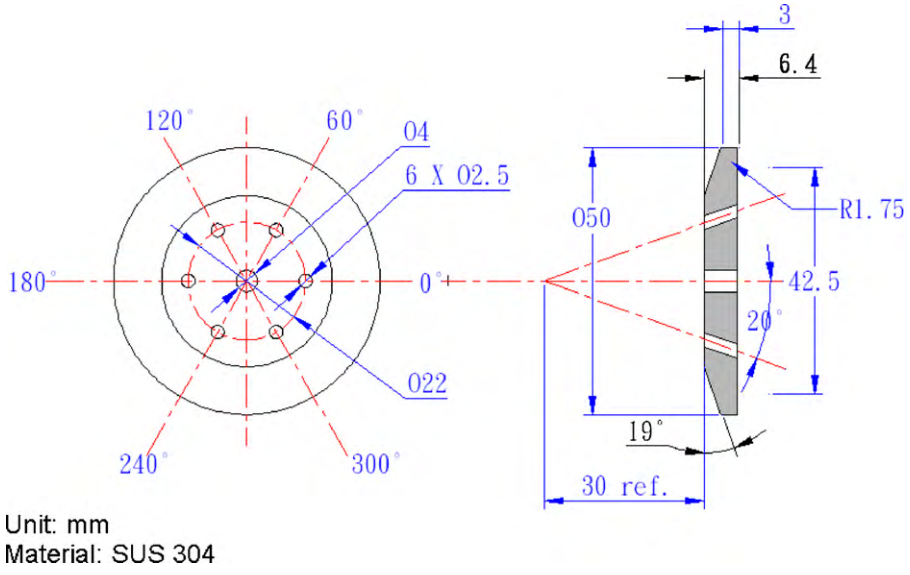

Fig. 2. Scheme of blowing nozzle.

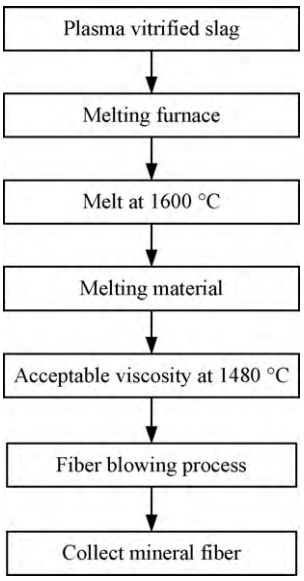

Fig. 3. Procedure for producing man-made vitreous fiber.

3.264 Pa s. The oxide melt stream is transported through the throat by gravity and blew with high pressure air (9 kg/cm^2) from a fiber blowing unit to produce mineral fiber and direct the fibers into collection equipment.

2.4. Measuring viscosity of molten slag

The liquid viscosity of vitrified slag can be measured between 1 and 10^5 Pa s using a Theta Industries Rheotronic II 1600 °C Rotating Viscometer. A mass of vitrified slag was placed in an alumina crucible with a weight of about 20 g and heated (under air; at 5 °C/min) well above its softening point in a vertical $MoSi_2$ resistance furnace under atmosphere. A rotating alumina spindle was lowered into the melt, producing a viscous drag on the spindle and the viscosity was measured using a Brookfield HBDV-III Ultra measuring head. Data are taken as a function of temperature to describe the viscosity–temperature relationship for the molten flux.

2.5. Determining shot content of product

According to ASTM C1335-04 [17], the specimen (10 g) was taken and fired at 593 ± 5.6 °C for 15 min. Dry sieve analysis method was applied to determine non-fibrous (shot) content of man-made slag mineral fiber. Three 203 mm diameter U.S.A. Standard Sieves (Nos. 20, 50 and 100) were nested in order and set on the motor-driven testing sieve shaker. The fired specimens were placed on the top sieve and an automatic shaker-hammer was operated for 20 min. Then, all the weighed material was retained on each sieve. Shot content were calculated using the following equation:

$$\text{Shot content } (\%) = \frac{\text{WP}}{\text{WT}} \times 100 \quad (1)$$

where WP = mass of material on all sieves (g) and WT = mass of specimen after firing (g).

2.6. Characterization methods of the MMVF

To assess the chemical resistance of MMVF, durability tests were performed in acid and alkaline water solutions. The acid solution was prepared by 10% H_2SO_4. The immersion time was 1.5 h and the temperature during the immersion was fixed at 80 ± 1 °C. The alkaline immersion test was conducted in an aqueous solution containing 2 mol/L of NaOH, boiled for 1 h and immersed for 3 h. Weight loss was then measured for evaluating chemical resistance.

The physical and chemical properties of fibers such as morphology, diameter, chemical resistance and shot content were also characterized in this study. The morphology and diameter of the fibers were analyzed by scanning electron microscopy (SEM) (S-4800; Hitachi, Japan).

2.7. Producing fiber-reinforced concrete

Fiber reinforcement concrete was made using Portland cement and mineral fibers. The water-to-solid ratio was 0.5. The mineral fiber was added in different quantities (0.2–1.5 wt.%) and the fiber was not treated in any form before being incorporated with concrete. The preparation was as follows. The mineral fibers were dispersed in the water at the beginning using soft paddle to avoid fiber balling and to produce the concrete with uniform material consistency and better workability. The optimal stirring time and speed were 10 min and 200 revolutions per minute, respectively. Then, the cement was placed in a stirred steel vessel where it was mixed for 5 min to form aqueous fiber-reinforced concrete slurry. The mixtures were poured into a steel cylinder mold to cast a standard 50 mm × 100 mm cylindrical concrete specimen for a compressive strength test and into a 40 mm × 40 mm × 160 mm steel prism mold for a flexural strength test. The specimens were consolidated using a vibrating table for 24 h, removed from the mold, and then cured in a programmable temperature and humidity chamber (at 23 ± 2 °C and 98% relative humidity) for 7 days and 28 days. Afterward, a compressive strength test and flexural strength test were conducted. For each test, at least five samples were tested and the results were averaged.

All the standard test cylinders were tested according to ASTM C39 [18] after 7 days and 28 days. The compressive test was executed in a 20 ton compression testing machine with a rate loading controller at a rate of 0.3 MPa/s until the load decreased to a value less than 95% of the peak load. Before testing, the cylinders were capped with a hard plaster on the cast face to ensure parallel loading faces of the specimens and fixed height for all test samples. The flexural strength was conducted under third-point loading in accordance with ASTM C 78-09 [19].

3. Results and discussion

3.1. Chemical compositions of vitrified slag

Because the incinerator ashes and vitrified slag were manufactured under an oxidative condition, the data of chemical compositions of them were shown as a percentage of oxide. Table 1 presents the primary chemical constituents in incinerator ashes and vitrified slag. The key remaining components were non-hazardous minerals, which were SiO_2, Al_2O_3, CaO and Fe_2O_3. The

Table 1
Major chemical constituents of fly ash, bottom ash and water-quenched vitrified slag.

	CaO (wt.%)	SiO_2 (wt.%)	Al_2O_3 (wt.%)	Fe_2O_3 (wt.%)	Na_2O (wt.%)	K_2O (wt.%)	Cl (wt.%)
Fly ash	46.91	12.56	8.23	1.85	5.78	2.36	17.65
Bottom ash	25.57	33.97	15.81	19.20	1.74	0.69	0.60
Water-quenched slag	25.52	38.31	12.27	11.22	2.08	3.42	0.0013

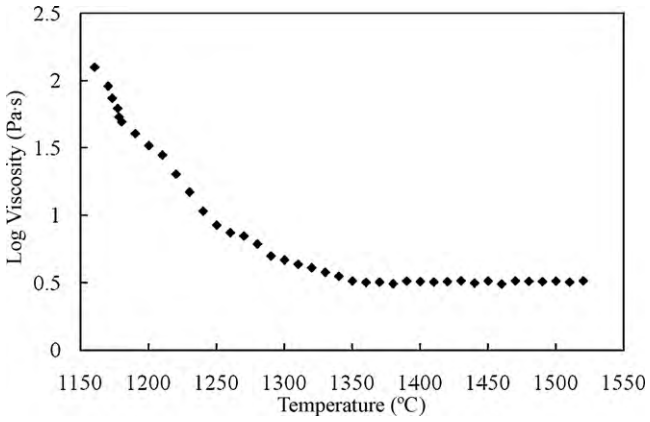

Fig. 4. Viscosity–temperature curve of molten vitrified slag.

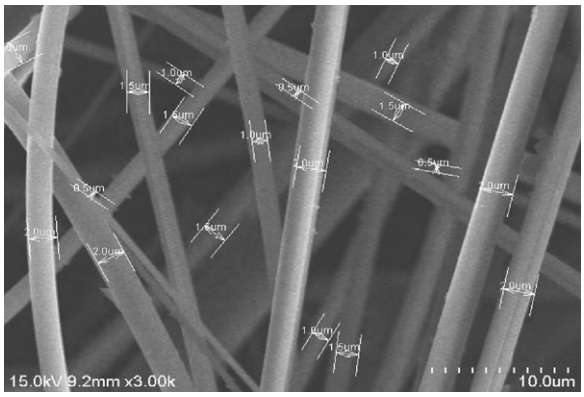

Fig. 5. SEM photomicrograph of blown man-made vitreous fiber.

oxides with high boiling points (such as SiO_2 and Al_2O_3) did not evaporate during vitrification and move into the water-quenched vitrified slag, so the percentage of these oxides was high. On the other hand, Na_2O, K_2O and Cl which have lower boiling points were evaporated in the plasma vitrification process and flowed into the air-pollution control system, where they were caught by the packed wet scrubber and bag house.

3.2. Viscosity of molten slag

The viscosity of the molten vitrified slag is plotted as a function of temperature in Fig. 4. Because the softening point of plasma vitrified slag was 1150 °C, the measurement was performed at 1160 °C. The curve in Fig. 4 shows the viscosity of molten vitrified slag decreases as the temperature is in the region of 1160–1520 °C and the slag was completely melted at about 1350 °C. The processing temperature and viscosity are 1480 °C and 3.264 Pa s, respectively. The processing temperature and viscosity are chosen because of their importance in various aspects of commercial, cost, workability and manufacturing of slag forming melts. At this processing condition, the viscous molten material would be homogeneous. Furthermore, it would be easily to convey the molten slag to the throat, and then blow with high velocity compressed air to produce MMVF.

3.3. Fibrous diameter and length

The resultant fiber pattern is a random mass of both straight and curled fibers intermingled with some variation in filament diameter and length because of the random nature of the fiber blowing process producing them. Fiber diameter is the most important factor as regards the specific performance for fiber and associated materials, since almost all major end-use behavior is determined by fiber diameter. For quality control of fiber sizes for blown fiber fabrication operation and providing accurate results, the diameter of the filament is extracted from the product and measured by SEM. The fiber patterns, orientation and filament diameter distribution are shown in Fig. 5. Sixteen fibers were measured to calculate the mean and standard deviation of fibrous diameters. The statistical measures of the distribution of fibrous diameters ranged from 0.5 to 2.0 μm. The arithmetic mean and standard deviation of fibrous diameter were 1.32 μm and 0.58, respectively. The fibers produced were several centimeters long, ranging from 1.5 to 5.0 cm.

3.4. Shot content of mineral fiber

As well as fibrous product, the fiber blowing process generates a large amount of round particles, mostly larger than 100 μm. This non-fibrous byproduct of the manufacturing process is determined that cannot be brushed or mechanically shaken through a No. 100 (150 μm) sieve. The arithmetic mean shot content and standard deviation are 11.042 wt.% and 3.687. The shot is often mobile, that is, not attached or adhered to adjoining fibers. Therefore, a cyclone unit was constructed to separate and remove non-fibrous material from the product. Fibrous product of 2.83 ± 2.02 wt.% shot content can be obtained following the separating process. The non-fibrous material does not contribute to the insulating value of the insulation; mechanical manipulation can be utilized to obtain higher quality output for insulating purposes.

3.5. Chemical resistance

The results of chemical resistance of MMVF before and after immersion are shown in Table 2. It can be seen the weight loss of MMVF after immersion in 10% H_2SO_4 aqueous solution were 1.12 wt.% of that before immersion. In contrast with acid solution, weight loss was 0.23 wt.% for MMVF in 2 mol/L NaOH solution. From the results, there is relatively higher weight loss for the acid durability test than that in alkali. The chemical durability test demonstrated MMVF has sufficient alkali resistance as a concrete-reinforcing fiber.

3.6. Effects of fibrous content on the compressive and flexural strength of concrete

Fig. 6 shows the relationship between the fibrous content and compressive strength of a 50 mm × 100 mm cylindrical concrete specimen. Both 7-day and 28-day compressive strength have similar variation tendencies versus fibrous content. When the fibers were introduced, it can be seen the compressive strength of specimens were increased compared to specimens produced without fibers. As the fibrous additive was 0.8 wt.%, the maximum compressive strength of both 7-day and 28-day specimens were reached, in which the strength was increased by 23% and 25%, and then declined slightly. The results of flexural strength tests of fiber-reinforced concrete are given in Fig. 7. Flexural strength also increases as the fibrous content increases and the slope of the ascending portion increases accordingly. Maximum strength was achieved at 0.8 wt.% fibrous. The enhancement of flexural strength was 25% for 7 days and 24% for 28 days, respectively. It is noticeable

Table 2
Chemical resistance for MMVF.

Chemical	Before test (g)	After test (g)	Weight loss (wt.%)
10% H_2SO_4	3	2.966	1.12
2 M NaOH	3	2.993	0.23

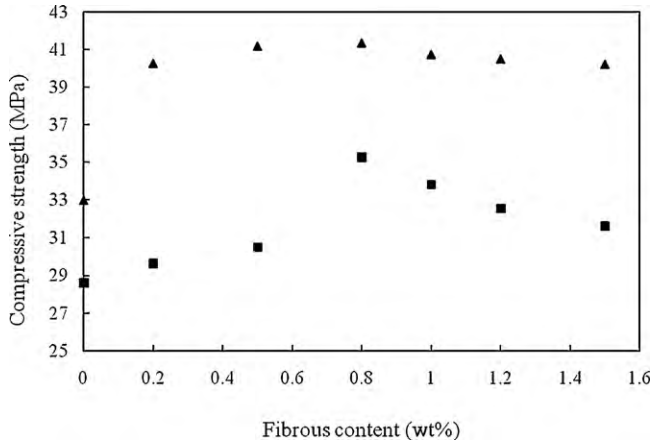

Fig. 6. Compressive strength of fibrous reinforcement concrete: (■) 7 days; (▲) 28 days.

at 0.2% fibrous content, the slope of the ascending trend increases sharply for both compressive and flexural strength. The 28-day strengths were 22% and 21% higher than non-fiber concrete, respectively.

The mineral fiber produced from this work was hydrophilic, promoting dispersion and suspension of fiber in mixing water and concrete slurry. The increased ability to distribute fibers throughout the concrete will distribute the unfavorable stress across a greater volume of concrete and improve the characteristics of fiber-reinforced concrete in the hardened state [13].

The MMVF in cement-based composites could be formed mechanical interlocking between their interfaces, have ability to transfer the forces by bonding and increase their fracture toughness which meant to improve resistance against cracking by prevent or control of crack opening, coalescence and propagation. When the load was increased to the cylindrical and prism concrete specimens, test samples were initiating to open cracks and advancing those cracks. The deboning, fiber fracture and fiber pull-out at fiber–cement interface were appeared while the progressing crack approached the fibers bridge. At this moment, the width of cracks was arrested and number of cracks was increased. Afterward post-cracking ductility was exhibited, allowed to resist additional stress, possessed high level of strain, delayed the final crushing of fiber-reinforced concrete and upgraded the mechanical strength over the unreinforced concrete.

The improved mechanical properties of MMVF were compared to that of conventional glass fiber. Glass fiber was also designed to introduce into cement-based materials and enhance their compressive and flexural strength. Conventional glass fiber must be treated and improved alkali resistance to apply in the relatively high pH environment of cement paste [20–22]. The MMVF produced in this work was no need to treat in any form before being incorporated with concrete. The enhancement of compressive strength of alkali resistant glass fiber-reinforced cement product was about 20% [21] and 23% [22] than unreinforced concrete for 28 days. The flexural strength was increased by about 32.5% [22] and 20% [23] for 28 days. In short, the enhancement of mechanical strength by MMVF was similar to that by glass fiber.

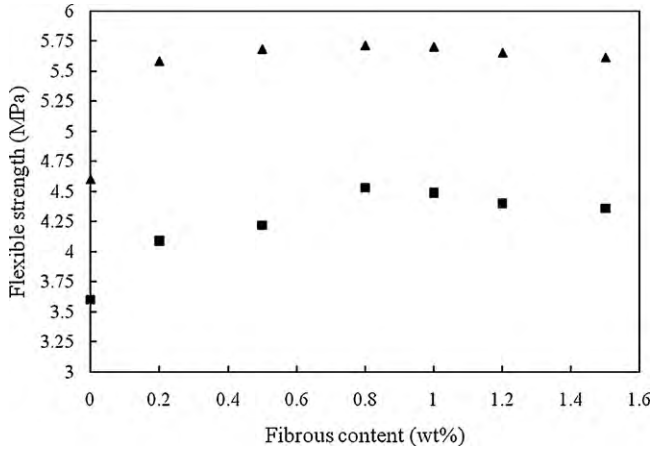

Fig. 7. Flexural strength of fibrous reinforcement concrete: (■) 7 days; (▲) 28 days.

4. Conclusions

In this study, the fiber blowing method was developed to produce MMVF to be utilized as reinforcement in concrete. The fibrous diameters and lengths range from 0.5–2.0 μm to 1.5–5.0 cm, respectively. Fibrous product of 2.83 ± 2.02 wt.% shot content can be obtained following the cyclone process. MMVF was also chemically resistant and suitable for use in concrete. In fiber-reinforced concrete tests, a proper fibrous content can improve the compressive and flexural strengths of the concrete. The improvements in the 28-day compressive and flexural strengths of fiber-reinforced concrete were 25% and 24%, respectively. The optimum additive was 0.8 wt.%.

The thermal plasma vitrification technique is suitable for treating municipal incinerator ash. Man-made vitreous fiber produced from slag as fiber reinforcement is a promising method for reutilizing incinerator ash. The findings from this work demonstrate that vitrified slag could be converted into a novel product. The reinforced mechanical properties of MMVF in comparison with alkali resistant glass fiber which was exploited in concrete applications, MMVF was competitively applied to cement as reinforcement. MMVF will be played an important role in successfully developing the plasma melting process if it can be on the market in the future.

References

[1] P. Appendino, M. Ferraris, I. Matekovits, M. Salvo, Production of glass–ceramic bodies from the bottom ashes of municipal solid waste incinerators, J. Eur. Ceram. Soc. 24 (2004) 803–810.
[2] K. Park, J. Hyun, S. Maken, S. Jang, J.W. Park, Vitrification of municipal solid waste incinerator fly ash using Brown's gas, Energy Fuel 19 (2005) 258–262.
[3] R.C.C. Monteiro, S.J.G. Alendouro, F.M.L. Figueiredo, M.C. Ferro, M.H.V. Fernandes, Development and properties of a glass made from MSWI bottom ash, J. Non-Cryst. Solids 352 (2006) 130–135.
[4] R.C.C. Monteiro, C.F. Figueiredo, M.S. Alendouro, M.C. Ferro, E.J.R. Davim, M.H.V. Fernandes, Characterization of MSWI bottom ashes towards utilization as glass raw material, Waste Manage. 28 (2008) 1119–1125.
[5] M. Bassani, E. Santagata, O. Baglieri, M. Ferraris, M. Salvo, A. Ventrella, Use of vitrified bottom ashes of municipal solid waste incinerators in bituminous mixtures in substitution of natural sands, Adv. Appl. Ceram. 108 (2009) 33–43.
[6] M. Ferraris, M. Salno, A. Ventrella, L. Buzzi, M. Veglia, Use of vitrified MSWI bottom ashes for concrete production, Waste Manage. 29 (2009) 1041–1047.
[7] S.F. Yang, W.T. Chiu, T.M. Wang, W.C. Lee, C.L. Chen, C.C. Tzeng, Asphalt concrete and permeable brick produced from incineration ash using thermal plasma technology, J. Environ. Eng. Manage. 19 (2009) 221–226.
[8] E. Gomez, D. Amutha Rani, C.R. Cheeseman, D. Deegan, M. Wise, A.R. Boccaccini, Thermal plasma technology for the treatment of wastes: a critical review, J. Hazard. Mater. 161 (2009) 614–626.
[9] H. Jimbo, Plasma melting and useful application of molten slag, Waste Manage. 16 (1996) 417–422.
[10] M. Nishigaki, Producing permeable blocks and pavement bricks from molten slag, Waste Manage. 20 (2000) 185–192.
[11] T.W. Cheng, M.Z. Huang, C.C. Tzeng, K.B. Cheng, T.H. Ueng, Production of coloured glass–ceramics from incinerator ash using thermal plasma technology, Chemosphere 68 (2007) 1937–1945.
[12] S.A. Ashour, F.F. Wafa, M.I. Kamal, Effect of the concrete compressive strength and tensile reinforcement ratio on the flexural behavior of fibrous concrete beams, Eng. Struct. 22 (2000) 1145–1158.
[13] P.S. Song, S. Hwang, B.C. Sheu, Strength properties of nylon- and polypropylene-fiber-reinforced concretes, Cem. Concr. Res. 35 (2005) 1546–1550.

[14] I.B. Topcu, M. Canbaz, Effect of different fibers on the mechanical properties of concrete containing fly ash, Constr. Build. Mater. 21 (2007) 1486–1491.
[15] T. Ochi, S. Okubo, K. Fukui, Development of recycled PET fiber and its application as concrete-reinforcing fiber, Cem. Concr. Compos. 29 (2007) 448–455.
[16] ASTM D1857-04, Standard Test Method for Fusibility of Coal and Coke Ash, 2004.
[17] ASTM C1335-04, Standard Test Method for Measuring Non-fibrous Content of Man-made Rock and Slag Mineral Fiber Insulation, 2009.
[18] ASTM C39/C39M-09a, Standard Test Method for Compressive Strength of Cylindrical Concrete Specimens, 2009.
[19] ASTM C78-09, Standard Test Method for Flexural Strength of Concrete (Using Simple Beam with Third-point Loading), 2009.
[20] S.L. Gao, E. Mader, A. Abdkader, P. Offermann, Sizings on alkali-resistant glass fibers: environmental effects on mechanical properties, Langmuir 19 (2003) 2496–2506.
[21] G. Barluenga, F. Hernandez-Olivares, Cracking control of concretes modified with short AR-glass fibers at early age. Experimental results on standard concrete and SCC, Cem. Concr. Res. 37 (2007) 1624–1638.
[22] W. Liang, J. Cheng, Y. Hu, H. Luo, Improved properties of GRC composites using commercial E-glass fibers with new coatings, Mater. Res. Bull. 37 (2002) 641–646.
[23] A. Sivakumar, M. Santhanam, Mechanical properties of high strength concrete reinforced with metallic and non-metallic fibres, Cem. Concr. Compos. 29 (2007) 603–608.